Physical and electrical characteristics of supramolecular polymer films based on guanosine derivatives modified with tetrathiafulvalene moiety

Seong Jib Choi, Junpei Kuwabara and Takaki Kanbara

Tsukuba Research Center for Interdisciplinary Materials Science (TIMS) Graduate School of Pure and Applied Sciences, University of Tsukuba, 1-1-1 Tennodai, Tsukuba 305-8573, (Japan), Fax: (+) 81-853-4490, E-mail: kanbara@ims.tsukuba.ac.jp

Supramolecular films consisting of guanosine derivatives modified with a tetrathiafulvalene (TTF) moiety have been prepared. The hydrogen bonding network of the guanosine unit enables the formation of a robust and self-supporting cast film by a solution process. Differential scanning calorimetry (DSC) and dynamic mechanical analysis (DMA) revealed that the self-supporting films were mechanically flexible and their glass transition temperature was lower than room temperature. The results of the DMA also showed the viscoelastic properties of the films at room temperature. The physical properties of the films of the derivatives depended on both the length of the alkyl chains and the structure of their terminal group. The chemical oxidation of the derivatives resulted in the formation of the absorption band due to the radical-cationic TTF moiety. The composite film of the derivatives with 7,7,8,8,-tetracyanoquinodimethane (TCNQ) exhibited electrical conductivity.

Keywords: 2-deoxyguanosine; electrical conductivity; hydrogen bond; supramolecular polymer; tetrathiafulvalene

INTRODUCTION

Tetrathiafulvalene (TTF) derivatives are well known organic π-donors. These molecules have received immense attention as electrically conducting materials.[1,2] TTF derivatives show electrical conductivity in the presence of oxidants in their crystalline state due to efficient interactions between π-orbitals leading to high mobility of charge carriers.[3] However, the charge-transfer (CT) complexes of TTF tend to be brittle and are therefore not suited to fabrication of practical macro-scale devices. Incorporation of TTF in a polymer structure is one of the simple strategies being investigated for solving this problem. Although various polymers with TTF moieties have been synthesized and characterized in terms of their electrical properties, most of these polymers exhibited low solubility or low electrical conductivity.[4-11] Self-organization of TTF using supramolecular interactions is regarded as another approach to produce one dimensional alignment of TTF with high electrical conductivity. The advantages of the supramolecular approach are the achievement of high solubility in the dispersed molecular state and highly ordered structure formation in the assembled solid state. There are several examples in material science of gel-like soft materials at the micro or nano scale, based on TTF molecules made via supramolecular interactions.[12-17] To obtain an increase in scale for applications, stronger intermolecular interactions are required in the structures of supramolecules with TTF. In previous work,[18] we have investigated guanosine derivatives containing a TTF moiety. Guanosine is a good candidate for forming a supramolecular polymer as it is capable of forming multiple hydrogen bonds with three hydrogen bonding acceptors and donors.[19-22] In addition, these hydrogen bonding networks tend to align the TTF moieties. The derivatives were expected to show polymeric properties due to the hydrogen bonding network, and electrical conductivity based on the CT complexes. In the present work, we report the systematic investigation of the physical and electrical properties of these supramolecular films.

EXPERIMENTAL PROCEDURE

Materials

The reagents were purchased from Tokyo Chemical Industry Co., Ltd., Kanto Chemical Co., INC., and Wako Pure Chemical Industries, Ltd., and were used without further purification. Anhydrous solvents were purchased from Kanto Chemical Co., INC. Column chromatography was carried out by using silica gel 60 (Kanto Chemical Co., INC., 40-100 μm, neutral). The guanosine derivatives **1-3** were synthesized by literature procedures.[18]

Synthesis of 4

3',5'-Bis-*O*-hexyloxy-di-*iso*-propylsilyl-2'-deoxyguanosine:

To a solution of triethylamine (0.27 mL, 2.0 mmol) and diisopropyldichlorosilane (0.72 mL, 4.0 mmol) in CH_2Cl_2 (15 mL) was added a solution of 1-hexanol (0.25 mL, 2.0 mmol) in CH_2Cl_2 (4.0 mL) at 0 °C. After the mixture was stirred for 3 h at 40 °C, the volatiles were

evaporated in vacuo. To the remaining crude product was added DMF (3.0 mL), imidazole (0.14 g, 2.0 mmol) and 2'-deoxyguanosine (0.13 g, 0.50 mmol). The mixture was stirred overnight at room temperature. The resulting solution was quenched with water. The organic material was extracted with ethyl acetate and dried over $MgSO_4$ and concentrated in vacuo. The residue was purified by column chromatography on silica-gel using ethanol/ethyl acetate (1 : 10 v/v) as an eluent (0.26 g, 75%). ^{1}H NMR (270 MHz, $CDCl_3$): δ 12.05 (br, 1H), 7.79, (s, 1H), 6.30-6.26 (m, 1H), 6.07 (br, 2H), 4.80-4.79 (m, 1H), 4.10-4.09 (m, 1H), 3.95-3.92 (m, 2H), 3.77-3.68 (m, 4H), 2.63-2.53 (m, 1H), 2.48-2.40 (m, 1H), 1.58-1.48 (m, 4H), 1.29-1.26 (m, 12H), 1.07-1.04 (m, 28H), 0.90-0.83 (m, 6H); ^{13}C{^{1}H} NMR (68 MHz, $CDCl_3$): δ 159.1, 153.3, 151.5, 135.6, 117.4, 88.0, 83.7, 72.2, 63.2, 63.2, 62.8, 41.3, 32.9, 32.8, 31.7, 25.5, 22.7, 17.5, 17.4, 14.1, 12.2, 12.1; ESI-MS: *m/z* calcd for $C_{34}H_{66}N_5O_6Si_2$ $[M+H]^+$: 696.5; found: 696.5; elemental analysis: calcd (%) for $C_{34}H_{65}N_5O_6Si_2$: C 58.67, H 9.41, N 10.06%; found: C 58.36, H 9.22, N 9.67%

Measurements

NMR spectra were recorded on a JEOL EX-270 NMR spectrometer. Elemental analyses were carried out with a Perkin-Elmer 2400-CHN instrument. ESI-Mass spectra were recorded on an Applied Biosystems QStar Pulsar *i* spectrometer. Absorption spectra were recorded using a Shimadzu UV-3100 spectrophotometer. ITO coated electrode (6.5~7.1 Ω•sq^{-1}, 2000 Å) was purchased from GEOMATIC. The electrical conductivities of cast films were measured by using a two-probe method at room temperature with ITO electrode fabricated by wet etching. X-ray diffraction patterns were recorded on a Philip X'Pert MRD with Cu*K*α radiation (λ = 1.542 Å) at a scanning rate of 0.088˚s $^{-1}$ in 2θ ranging 2.5˚ to 60˚ at room temperature. The self-supporting films were fabricated by a solvent-cast method using 0.1 M solution in THF on a glass plate (18 mm × 18 mm). The thermal properties were measured on SII EXSTAR6200 DSC instruments and a EXSTAR TG/DTA6300 instrument. The tensile strength of the self-supporting film was measured by a RSA-G2 (TA Instruments) at 25 °C. The dynamic mechanical measurements were conducted using a Q800 Dynamic Mechanical Analyzer (TA Instruments) at single-frequency scanning mode of 1 Hz and a cooling rate of 1 °C / min over a temperature range from 25 °C to -100 °C. Amplitude of 0.1% was used in the film (14.83 (L) mm × 4.00 (W) mm × 0.07 (T) mm).

RESULTS AND DISCUSSION

Derivatives **1**, **2**, and **3** were synthesized according to literature procedures (Figure 1).[18] Derivative **4** without a TTF moiety was synthesized as a control in order to evaluate the effect of the TTF moiety in terms of self-assembly and physical properties.

<Figure 1>

The syntheses of the derivatives proceeded efficiently without the need for a protecting process on the guanine moiety and chemical oxidation of the TTF moiety was seen not to occur during the reactions. The hydrogen bonding of the derivatives was confirmed by proton nuclear magnetic resonance spectroscopy (^{1}H NMR). The ^{1}H NMR signals of NH and NH_2 in the guanosine moiety shifted downfield with increasing concentration or decreasing temperature. Similar shifts were observed for all of the derivatives. These tendencies were consistent with those of reported hydrogen bond networks of guanosine derivatives in the solution state.[14,18,23,24] Due to the hydrogen bonding network, it was hypothesized that it would be possible to fabricate a polymer-like film from these materials.[23] Indeed, the fabrication of macroscale cast films was achieved by a solvent-casting method on a glass plate. The cast film was fabricated from a 0.1 M solution of derivatives **1**-**4** in tetrahydrofuran or chloroform on a glass plate. Based on the NMR observations, the formation of the films was attributed to the hydrogen bonding network of the guanine units.[23-26]

<Figure 2>

Figure 2 shows photographs of the films synthesized from guanosine derivatives **1**-**4**. It can be seen that the films possessed adequate strength to form self-supporting structures. The film of derivative **1** was stiff, whereas the films of derivatives **2**, **3**, and **4** were flexible. These observations suggest that the length of the alkyl chains affects the physical properties of the films.

Thermodynamical and mechanical properties

The thermal stability of derivatives **1**-**4** was evaluated by thermogravimetry analysis (TGA). Below 200 °C, no loss of weight was observed, which indicated that solvent molecules were not contained in the solid state (Figure S1). The elemental analyses, differential scanning calorimetry (DSC), and ^{1}H NMR spectroscopy also suggested that the derivatives did not contain solvent molecules. Therefore, the self-supporting films appeared to be constructed by hydrogen bonding without the assistance or incorporation of solvent molecules. The 5% weight loss temperatures ($T_{d5\%}$) of derivatives **1**-**4** were 225.4, 241.1, 256.4, and 249.9 °C, respectively (Table 1). The thermal stability of the TTF-substituted derivatives increased with the alkyl chain length (**1** < **2** < **3**). High thermal stability of the derivative with the long alky chains is attributed to a high content of heat-resistant alkyl chains in molecular weight. The thermal stability of derivative **4** was comparable to that of derivative **2**, which has an alkyl chain of similar length. To obtain detailed information on the thermal properties of the derivatives, DSC measurements were carried out on the basis of the TGA data (Figure S2). Table 1 summarizes the thermal properties of the derivatives **1**-**4**.

<Table 1>

In the first DSC heating run, derivatives **1**-**4** exhibited only endothermic peaks at 122, 95.1, 75.2, and 162°C, respectively. These peaks were assigned to the solid-to-liquid phase change of the substances (T_m). The curves obtained from the second DSC heating run of derivatives **1**-**4** showed gentle slopes at -1.2, -4.6, -21, and -52 °C, respectively. These slopes were attributed to a glass transition (T_g). In addition, exothermic peaks were observed at around 10 °C, which was considered to be the crystallization temperatures (T_c) of these derivatives. The existence of T_cs indicates that the derivatives have both the amorphous and crystalline phases that are often observed in conventional polymers. Because T_g and T_c are lower than room temperature, derivatives **1**-**4** seem to be polymer-like at this temperature. The T_m and T_g of the TTF-substituted derivatives shifted to lower temperatures with increasing alkyl chain length. These results suggest that the thermal properties of the derivatives depend on alkyl chain length. The T_g of derivative **2** was higher than that of derivative **4** even though they have alkyl chains of a similar length. This was attributed to the presence of the large TTF terminal unit.[27] In repeated DSC heating runs, the T_ms of the derivatives shifted to lower temperatures. As the ^{1}H NMR spectra showed no apparent decomposition of the derivatives after DSC analysis, the shifts of T_m were probably caused by changes in intermolecular interactions in the film state via thermal treatments.[21]

To evaluate the polymer-like properties of the materials, the tensile strength of the self-supporting films of derivatives **2**-**4** was measured using the tensile testing mode of dynamic mechanical analysis (DMA). Table 2 summarizes the mechanical properties. The tensile strength of derivative **1** could not be measured due to the brittleness of its film. The tensile strengths of derivatives **2**-**4** were 1.2, 0.19, and 2.5 MPa at the breaking point with elongation percentages at 25 °C of 23, 20, and 2.7 %, respectively (Table 2). The decrease in tensile strength of the self-supporting film of **3** compared to that of **2** is attributed to the longer alkyl chain. However, the tensile strength of derivative **4** was larger than that of derivative **2** even though they had alkyl chains of a similar length. These results indicate that the absence of the TTF moiety strengthened the intermolecular interaction between the alkyl chains of derivative **4**.

<Table 2>

We also investigated the polymer-like properties of the self-supporting films using the dynamic modulus mode of DMA (Figure 3). The DMA curves of the derivatives were similar to those of representative viscoelastic polymers.[28-30]

<Figure 3>

The storage modulus (E') of all of the derivatives decreased with increasing temperature and was higher than the loss modulus (E'') at all temperatures tested (Figure S3). These results suggest that the physical properties of the self-supporting films are solid-like.[29] Because the E' of derivative **4** (184 MPa) was larger than that of derivative **2**, (8.28 MPa) even though their alkyl chains were similar in length, it appears that the van der Waals forces between the simple alkyl chains were stronger than those between the alkyl chains with TTF as the terminal group at 25 °C. The maximum point of a tan delta curve (E''/E') indicates the T_g.[28.29] From the maximum points of the tan delta listed in Table 2, the T_g values of derivatives **2**-**4** were estimated to be -3.7, -19, and -51 °C, respectively. These values of T_g were consistent with those obtained using DSC. Because the values of tan delta indicated fluidity of the films, the materials were also evaluated using tan delta at T_g. Based on the tan delta values, derivatives **2** and **3** were seen to have a similar fluidity, whereas derivative **4** had low fluidity. This trend is consistent with the elongation percentage values measured during the tensile tests (Table 2). These results suggest that the terminal units play an important role in determining the physical properties of the films.

Chemical oxidation of TTF moieties

<Figure 4>

We previously reported the electrochemical properties of the TTF moiety of derivatives **1**-**3** as measured using cyclic voltammetry.[18] Derivatives **1**-**3** were seen to have two reversible redox peaks. To evaluate the oxidation of the TTF moiety, various chemical oxidations of derivative **3** were carried out in the solution state. UV-Vis absorption spectra of **3** with various oxidants exhibited the characteristic absorption band of the oxidized TTF moieties (Figure 4). Upon the addition of two equivalents of oxidants to derivative **3**, new absorption bands appeared at 580, 530 and 430 nm. The absorption bands were assigned to the mono-oxidized TTF moieties ($TTF^{+\bullet}$).[29,30] Furthermore, the oxidized form of derivative **3** exhibited a strong absorption band with a maximum at 760 nm. According to the literature,[33] the UV-Vis absorption at around 760 nm is assigned to a dimer structure of the mono-oxidized TTF moieties. Therefore, the oxidation of derivative **3** caused the formation of a stacked structure of the TTF moieties in solution. Because the absorption band at 760 nm was observed even in a dilute solution, the intramolecular interactions of mono-oxidized TTF moieties were dominant. Owing to the high oxidation potential of nitrosonium tetrafluoroborate ($NOBF_4$), the chemical oxidation of TTF moieties proceeded quantitatively, whereas other oxidants such as iron (III) chloride ($FeCl_3$) and iodine (I_2) were less effective.

<Figure 5>

The stepwise chemical oxidation of derivative **3** with $NOBF_4$ can be monitored by UV-Vis spectroscopy (Figure 5). Upon the addition of $NOBF_4$, the absorption band of the oxidized TTF moiety at 760 nm increased until the amount of oxidant reached two equivalents. The addition of four equivalents of $NOBF_4$ decreased the absorption of the stacked [$TTF^{+\bullet}$], and a new absorption band appeared at 360 nm. This band was assigned to dicationic TTF moieties ([TTF^{2+}]).[31,32] These results suggest that the decrease in the intensity of the absorption band at 760 nm is attributed to disaggregation of the stacked TTF moieties because of repulsive force in [TTF^{2+}].

Electrical conductivity

Table 3 summarizes the electrical conductivity of cast films of **1**, **2** and **3** under various conditions.[18] The films exhibited no electrical conductivity in their native state, whereas oxidation of the TTF moieties with 7,7,8,8,-tetracyanoquinodimethane (TCNQ) induced a degree of electrical conductivity in the films (entries 1 and 2).

<Table 3>

Derivatives **2** and **3** treated with TCNQ exhibited electrical conductivities of 1.00×10^{-2} and 3.66×10^{-2} $S \bullet cm^{-1}$, respectively. However, the oxidized film of derivative **1** exhibited no electrical conductivity. When tetracyanoethylene (TCNE), I_2, $NOBF_4$, silver tetrafluoroborate ($AgBF_4$), $FeCl_3$, and acetylferrocenium tetrafluoroborate (Fe^{3+}) were used as oxidants, no electrical conductivity was observed even though the oxidation of TTF moiety could be confirmed by the color change (entries 5-10). These results suggest that the alignment of the TTF moieties of derivatives **2** and **3** with TCNQ is different from those with the other oxidants in the films.

<Figure 6>

To investigate the alignment of the TTF moieties, powder X-ray diffraction (XRD) measurements of the oxidized cast films were carried out (Figure 6). As shown in Figure 6a, the TTF moiety of the derivative **3** exhibited no apparent diffraction pattern in a neutral condition.[18] The observed weak diffraction pattern indicates the presence of a lamellar-like structure constructed by the hydrogen bonding network of the guanosine moieties[25,26,34] because derivative **4** without a TTF moiety also exhibited a weak diffraction pattern. The

diffraction patterns of **3** and **4** were somewhat different suggesting different alignments of the hydrogen bonding networks (Figure S4e).[34,35] In the film of derivative **3** oxidized using TCNQ (entry 2, Table 4), a sharp reflection appeared at 10.9 (d = 8.19 Å) with higher-order reflections at 21.9 and 33.1, indicating a high degree of crystallinity (Figure 6b). The sharpness and position of the reflections are consistent with of those of the TTF-TCNQ CT complex in a thin film state.[36] The film of oxidized derivative **3** is likely to contain similar segregated one-dimensional chain alignment of the TTF moiety and TCNQ molecule. In contrast, the films of derivative **3** oxidized with I_2, TCNE, $NOBF_4$ or $FeCl_3$ did not exhibit a sharp reflection (Figure 6c-f)[18]. These results indicate that the TTF moiety and the anion section do not form a periodic structure, such as segregated one-dimensional chains, which is a reasonable explanation for the lack of electrical conductivity (entries 5-8, Table 4). In the film of **2** oxidized with TCNQ, similar sharp reflections were observed. However, the film of **1** oxidized with TCNQ exhibits reflections due to crystals of TCNQ as well as the reflections due to the TTF-TCNQ complex (Figure S4). The existence of TCNQ crystals suggests incomplete oxidation of the TTF moiety. Consequently, the electrical conductivity of the derivatives in the solid state strongly depends on the periodic alignment of the CT complex of the TTF moiety with TCNQ.

CONCLUSION

In this work, we synthesized guanosine derivatives with a TTF moiety. The guanosine derivatives formed strong hydrogen bonding networks and could be fabricated into self-supporting films. The films of the derivatives had similar physical properties to those of representative viscoelastic polymers in terms of tensile strength and viscoelasticity, and this was attributed to the hydrogen bonding networks present in the solid state. Both the length and the terminal group of the alkyl chains affected the physical properties. The long alkyl chain of the derivatives is one of the origins of the flexibility of the films. The self-assembled guanosine derivatives with a TTF moiety in the presence of TCNQ underwent one dimensional alignment of the TTF-TCNQ CT complex in the film state. Taking advantage of this supramolecular approach, electrically conducting films can be fabricated on the macro scale by a simple solution process.

ACKNOWLEDGEMENTS

This work was partly supported by Grants-in-Aid for Scientific Research from the Ministry of Education, Culture, Sports, Science and Technology, Japan. The Circle for the promotion of science and Engineering is acknowledged for the financial support. The authors are grateful to the Chemical Analysis Center of University of Tsukuba for elemental analyses and NMR spectroscopy. The authors grateful thank to Mr. T. Aikawa and Mr. J. Kanai in TA Instruments for the measurements of DMA. Prof. Y. Otsuka and Mr. Y. Shoji are acknowledged for technical supports of the measurements of electrical conductivity.

Supplementary information is available at Polymer Journal's website

1 Ferraris, J., Cowan, D. O., Walatka, Jr. V. & Perlstein, J. H. Electron transfer in a new highly conducting donor-acceptor complex *J. Am. Chem. Soc*. **95**, 948-949 (1973).

2 Alves, H., Molinari, A. S., Xie, H. & Morpurge, A. F. Metallic conduction at organic charge-transfer interfaces *Nature Mater.* **7**, 574-580 (2008).

3 Perlstein, J. H. "Organic Metals"-The intermolecular migration of aromaticity *Angew. Chem. Int. Ed. Engl.* **16**, 519-534 (1977).

4 Inagi, S., Naka, K. & Chujo Y. Functional polymers based on electron-donating TTF and derivatives *J. Mater. Chem.* **17**, 4122-4135 (2007).

5 Hertler, W. R. Charge-transfer polymers containing 7,7,8,8-tetracyanoquinodimethan and tetrathiafulvalene *J. Org. Chem.* **41**, 1412–1416 (1976).

6 Green, D. C. & Allen, R. W. Vinyltetrathiafulvalene *J. Chem. Soc., Chem. Commun.* 832–833 (1978).

7 Kaplan, M. L., Haddon, R. C., Wudl, F. & Feit, E. D. Preparation of some monophenyltetrathiafulvalenes and (*p*-vinylphenyl)tetrathiafulvalene and its polymerization *J. Org. Chem.* **43**, 4642–4646 (1978).

9 Pittman, C. U. Jr., Ueda, M. & Liang, Y. Syntheses of poly(urethanes) and poly(sulfonates) containing tetrathiafulvalene nuclei in the backbone *J. Org. Chem.* **44**, 3639–3642 (1979).

10 Frenzel, S. Arndt, S., Gregorious, R. M. & Müllen, K. Synthesis of tetrathiafulvalene polymers *J. Mater. Chem.* **5**, 1529–1537 (1995).

11 Shimizu, T. & Yamamoto, T. Preparation of a new poly(arylacetylene) with a tetrathiafulvalene (TTF) unit in the side chain *Chem. Commun.* 515–516 (1999).

12 Iyoda, M., Hasegawa, M. & Enozawa, H. Self-assembly and nanostructure formation of mulkti-funtional organic π-donors *Chem. Lett.* **36**, 1402-1407 (2007).

13 Naka, K., Ando, D., Wang, X. & Chujo, Y. Synthesis of organic-metal hybrid nanowires by cooperative self-organization of tetrathiafulvalene and metallic gold via charge-transfer *Langmuir* **23**, 3450-3454 (2007).

14 Kitahara, T., Shirakawa, M., Kawano, S., Bejinn, U. Fujita, N. and Shinkai, S. Creation of a mixed-valence state from one-dimensionally aligned TTF utilizing the self-assembling nature of a low molecular-weight gel *J. Am. Chem. Soc.* **127**, 14980-14981 (2005).

15 Kitamura, T., Nakaso, S., Mizoshita, N., Tochigi, Y., Shimomura, T., Moriyama, M., Ito, K. & Kato, T. Electroactive supramolecular self-assembled fibers comprised of doped tetrathiafulvalene-based gelators *J. Am. Chem. Soc.* **127**, 14769-14775 (2005).

16 Tatewaki, Y., Hatanaka, T., Tsunashima, R., Nakamura, T., Kimura, M. & Shirai, H. Conductive nanoscopic fibrous assemblies containing helical tetrathiafulvalene stacks *Chem. Asian. J.* **4**, 1474-1479 (2009).

17 Hasegawa, M., Enozawa, H., Kawabata, Y. & Iyoda, M. Hexagonally Ordered Nanostructures Comprised of a flexible disk-like molecule with high self-assembling

properties at neutral and cationic states *J. Am. Chem. Soc.* **129**, 3072–3073 (2007).
18 Choi, S. J., Kuwabara, J., Kanbara, T. Electrically Conductive hydrogen-bond-based supramolecular polymer with tetrathiafulvalene moiety: modulation of electrical conductivity and flexibility of film by external stimulus *Chem. Asian J.* **5**, 2154-2157 (2010).
19 Davis, J. T. & Spada, G. P. Supramolecular architectures generated by self-assembly of guanosine derivatives *Chem. Soc. Rev.* **36**, 296-313 (2007).
20 Araki, K. & Yoshikawa, I. Nucleobase-containing gelators *Top. Curr. Chem.* **256**, 133-165 (2005).
21 Yoshikawa, I., Li, J., Sakata, Y. & Araki, K. Design and Fabrication of a Flexible and Self-Supporting Supramolecular Film by Hierarchical Control of the Interaction between Hydrogen-Bonded Sheet Assemblies *Angew. Chem., Int. Ed.* **43**, 100-103 (2004).
22 Araki, K., Takasawa, R. & Yoshikawa, I. Design, fabrication, and properties of macroscalesupramolecular fibers consisted of fully hydrogen-bonded pseudo-polymerchains *Chem. Commun.* 1826-1827 (2001).
23 Gottarelli, G., Masiero, S., Mezzina, E., Pieraccini, S., Rabe, J. P., Samorì, P. & Spada, G. P. The self-assembly of lipophilic guanosine derivatives in solution and on solid surfaces *Chem. Eur. J.* **6**, 3242-3248 (2000).
24 Spada, G. P., Lena, S., Masiero, S., Pieraccini, S., Surin, M. & Samorì, P. Guanosine based H-bonded scaffolds: controlling the assembly of oligothiophenes *Adv. Mater.* **20**, 2433-2438 (2008).
25 Yoshikawa, I., Yanagi, S., Yamaji, Y. & Araki, K. Nucleoside-based organogelators: gelation by the G-G base pair formation of alkylsilylated guanosine derivatives *Tetrahedron* **63**, 7474-7481 (2007).
26 Takasawa, R., Yoshikawa, I. & Araki, K. Use of an adjustable soft segment as an effective molecular design for crystal engineering of hydrogen-bonded tape motifs *Org. Biomol. Chem.* **2**, 1125-1132 (2004).
27 Tanaka, K., Ishiguro, F. & Chujo Y. Facile preparation of concentration-gradient materials with radical spin of the mixed-valence tetrathiafulvalene in conventional polymer films *Langmuir* **26**, 10254–10258 (2010)
28 Bower, D. I. An introduction to polymer physics (Cambridge University Press, New York, 2002)
29 Menard, K. P. Dynamic mechanical analysis: A practical introduction, 2nd Edition, (CRC Press, Boca Raton, 2008)
30 Gosline, J., Lille, M., Carrington, E., guerette, P., Ortlepp, C. & Savage, K. Elastic proteins biological role and mechanical properties *Phil. Trans. R. Soc. Lond. B* **357**, 121-132 (2002).
31 Zhou, Y., Wu, H., Qu, L., Zhang, D. & Zhu, D. A new redox-resettable molecule-based half-adder with tetrathiafulvalene *J. Phys. Chem. B* **110**, 15676-15679 (2006).
32 Torrance, J. B., Scott, B. A. Welber, B., Kaufman, F. B. & Seiden, P. E. Optical properties of the radical cation tetrathiafulvalenium (TTF^{+}) in its mixed-valence and monovalence halide salts *Phys. Rev. B* **19**, 730–741 (1979).
33 Ziganshina, A. Y., Ko, Y. H., Jeon, W. S. & Kim, K. Stable π-dimer of a

tetrathiafulvalene cation radical encapsulated in the cavity of cucurbit[8]uri *Chem. Commun.* 806-807 (2004).

34. Yoshikawa, I., Sawayama, J. & Araki, K. Highly stable giant supramolecular vesicles composed of 2D hydrogen-bonded sheet structures of guanosine derivatives *Angew. Chem. Int. Ed.* **47**, 1038 –1041 (2008).
35. Giorgi, T., Grepioni, F., Manet, I., Mariani, P., Masiero, S., Mezzina, E., Pieraccini, S., Saturni, L., Spada, G. P. & Gottarelli, G. Gel-like lyomesophases formed in organic solvents by self-assembled guanine ribbons *Chem. Eur. J.* **8**, 2143-2151 (2002)

36 Fraxedas, J., Molas, S., Figueras, A., Jiménez, I., Gago, R., Auban-Senzier, P. & Goffman, M. Thin films of molecular metals: TTF-TCNQ *J. Solid State Chem.* **168**, 384-389 (2002).

[Figure Legend]

Figure 1 Structure of the guanosine derivatives **1**-**4**.

Figure 2 Self-supporting films of the derivatives a) **1**, b) **2**, c) **3**, and d) **4**; the size of all derivatives is 18 × 18 mm, except for derivative **1**.

Figure 3 Dynamic mechanical analysis curves of the self-supporting film of derivative **3**;(- - storage modulus (E'), ••• loss modulus (E''), — Tan $\delta = E'' / E'$; single-frequency scanning mode of 1 Hz, cooling rate of 1 °C/min)

Figure 4 UV-Vis absorption spectra of derivative **3** in 0.02 mM $CHCl_3$ solution, and **3** with two equivalent of various oxidants; **3** (broken line, — —), **3** + $NOBF_4$ (diamond line, —◆—), **3** + $FeCl_3$ (cycle line, —○—), **3** + I_2 (triangle line, —▲—).

Figure 5 UV-Vis absorption spectra of derivative **3** (0.02 mM solution in $CHCl_3$) with various amounts of $NOBF_4$; **3** (broken line, — —), **3** + 0.5 eq. $NOBF_4$ (square line, —■—), **3** + 1. 0 eq. $NOBF_4$ (triangle line, —△—), **3** + 2.0 eq. $NOBF_4$ (diamond line, —◆—), **3** + 4.0 eq. $NOBF_4$ (cross line, —╳—).

Figure 6 Powder X-ray diffraction patterns of cast films of oxidized derivative **3**; a) **3**,[18] b) **3**+TCNQ,[18] c) **3**+I_2,[18] d) **3**+2.0 eq. TCNE,[18] e) **3**+2.0 eq $NOBF_4$, and f) **3**+2.0 eq $FeCl_3$.

[Table Legend]

Table 1 The thermal properties of derivatives **1**-**4**

[a] Temperature for 5.0% thermal decomposition obtained by TGA (heating rate of 10 °C / min, argon atmosphere), [b] Glass transition temperature obtained by DSC curve of second heating run, [c] Phase transition temperature obtained by DSC of second heating run, [d] Melting point on the fist heating run of DSC, [e] Melting point on the third heating run of DSC.

Table 2 The mechanical properties of the films of derivatives **2**-**4**

[a] Tensile strength of self-supporting film, [b] Elongation of break point in tensile test, [c] Storage modulus (E') at 25 °C, [d] Loss modulus (E'') at 25 °C, [e] Glass transition temperature obtained by DMA, [f] Tan δ (= E'' / E') at glass transition temperature.

Table 3 Electrical conductivities of derivatives **1**-**3**

[a] Electrical conductivity of the cast film from THF solution was determined by two-probe technique at room temperature, [b] Previous work, [c] Acetylferrocenium tetrafluoroborate, [d] Not determined due to low electrical conductivity.

SUPPLEMENTARY INFORMATION

Physical and electrical characteristics of supramolecular polymer films based on guanosine derivatives modified with tetrathiafulvalene moiety

Seong Jib Choi, Junpei Kuwabara and Takaki Kanbara

Tsukuba Research Center for Interdisciplinary Materials Science (TIMS) Graduate School of Pure and Applied Sciences, University of Tsukuba, 1-1-1 Tennodai, Tsukuba 305-8573, (Japan), Fax: (+) 81-853-4490, E-mail: kanbara@ims.tsukuba.ac.jp

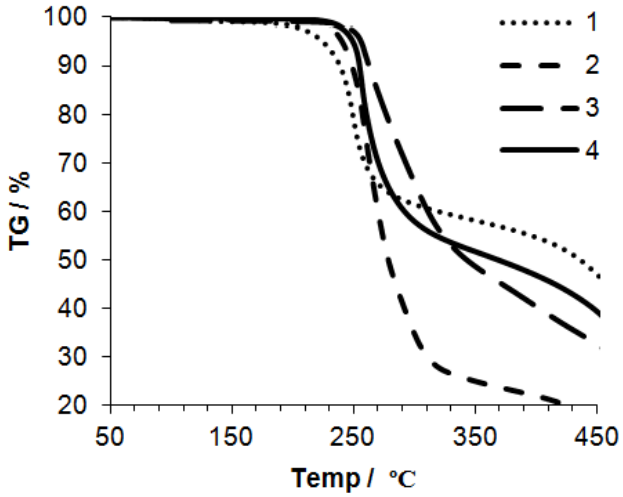

Figure S1 Thermogravimetry analysis curves of the derivatives **1**-**4**.

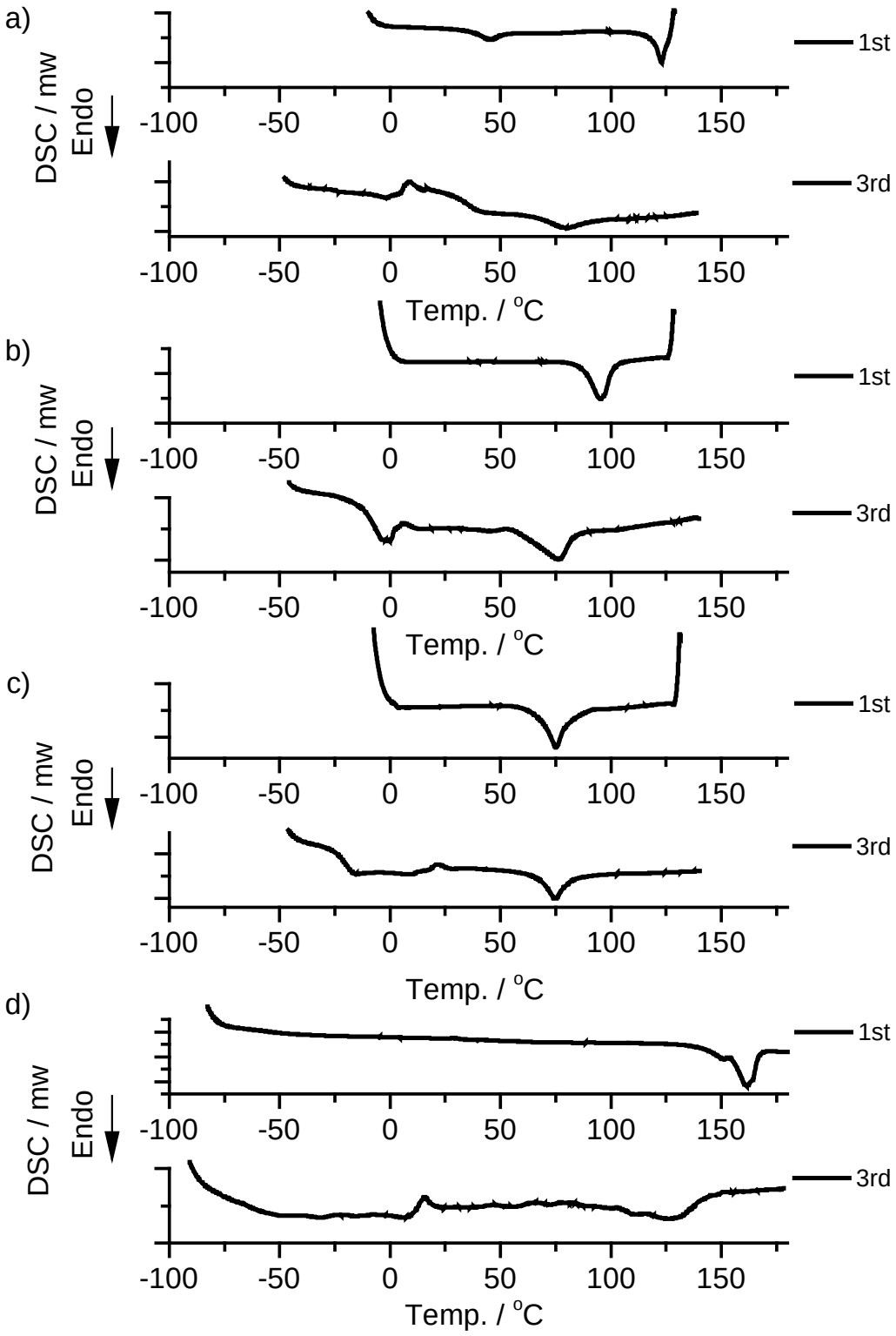

Figure S2 The differential scanning calorimetric curves of the derivatives **1**-**4** at the first and third heating run (heating rate of 10 ºC / min, argon atmosphere); a) **1**, b) **2**, c) **3**, and d) **4**.

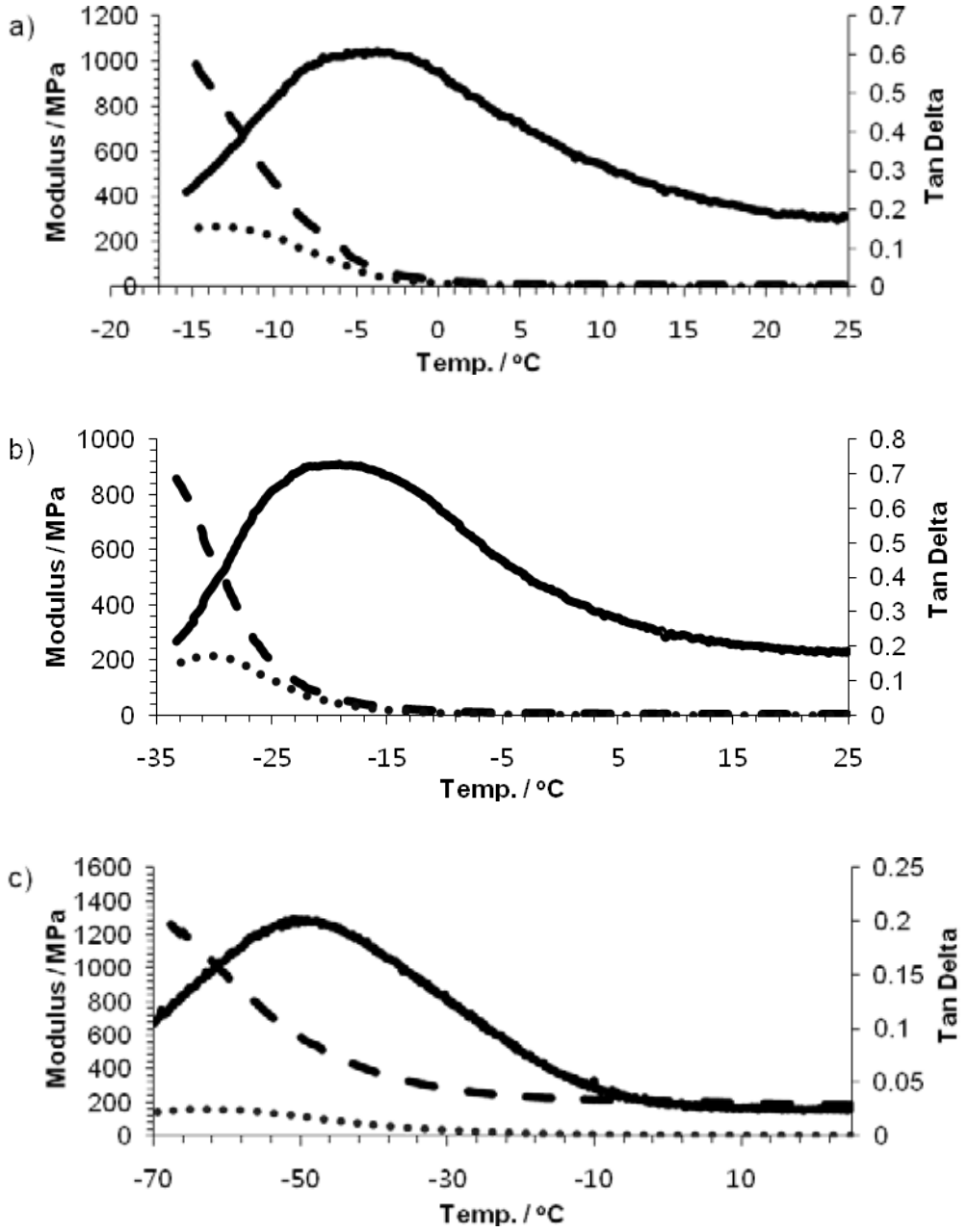

Figure S3 The dynamic mechanical analysis curves of self-supporting films; a) **2**, b) **3**, and c) **4**. (- - The storage modulus (E'), ••• The loss modulus (E''), — Tan $\delta = E'' / E'$; single-frequency scanning mode of 1 Hz, cooling rate of 1 ºC /min)

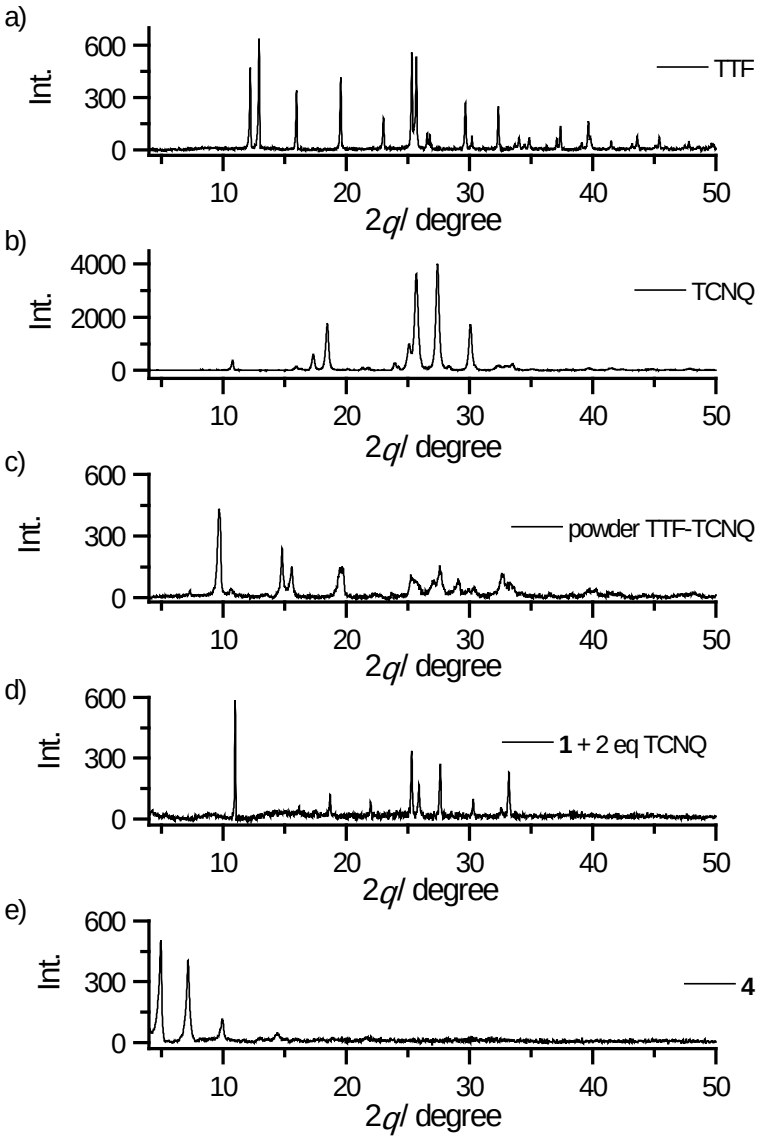

Figure S4 Powder X-ray diffraction patterns of a) TTF, b) TCNQ, c) powder TTF-TCNQ, d) derivative **1** + 2 eq. TCNQ and, e) powder-XRD of derivative **4**.

[Graphical Abstract]

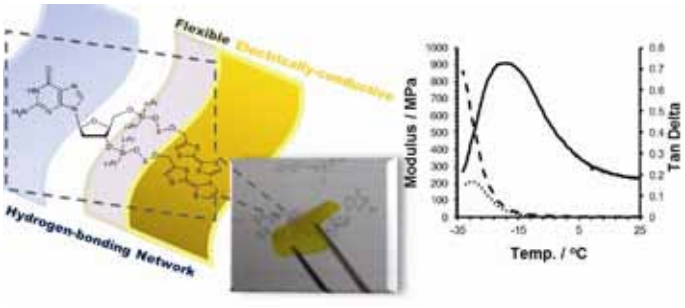

Supramolecular films consisting of guanosine derivatives modified with a tetrathiafulvalene (TTF) moiety have been prepared. The hydrogen bonding network of the guanosine unit enables the formation of a robust and self-supporting cast film by a solution process. The self-supporting films were mechanically flexible. The physical properties of the films of the derivatives depended on both the length of the alkyl chains and the structure of their terminal group. The composite film of the derivatives with 7,7,8,8,-tetracyanoquinodimethane (TCNQ) exhibited electrical conductivity.

Fig.1

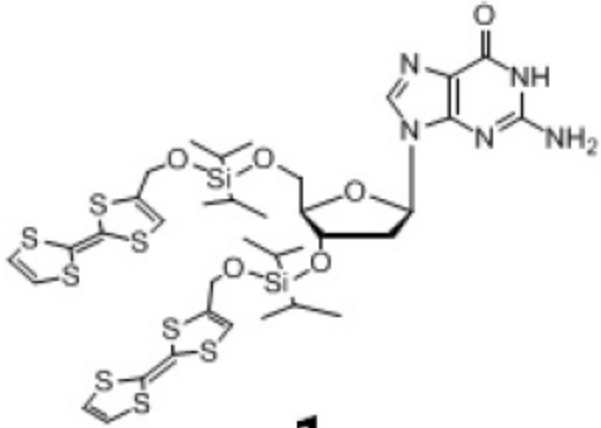

1

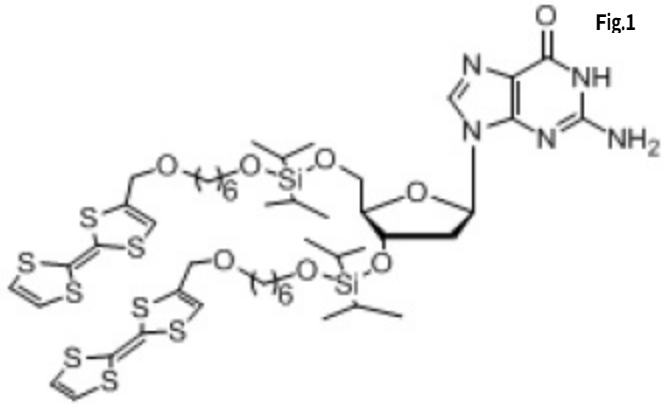

2

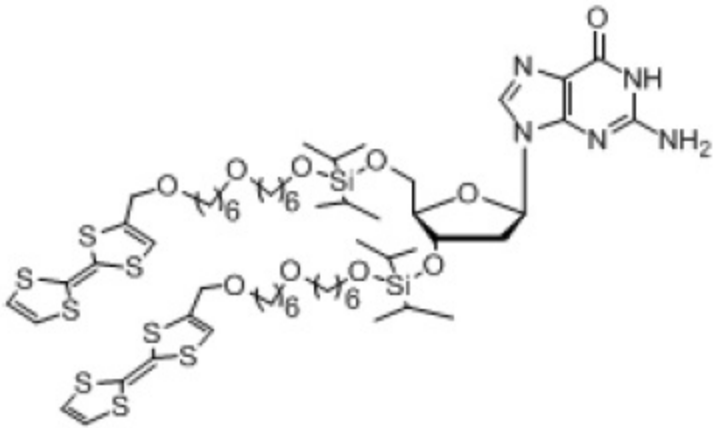

3

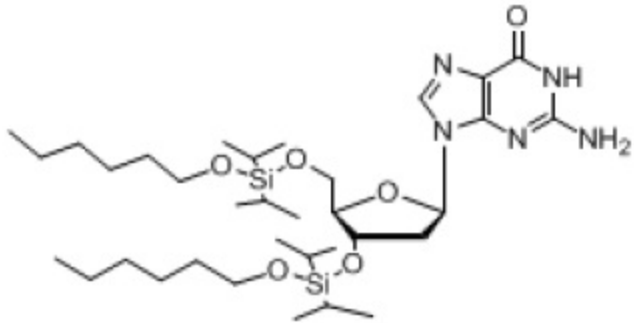

4

Fig.2

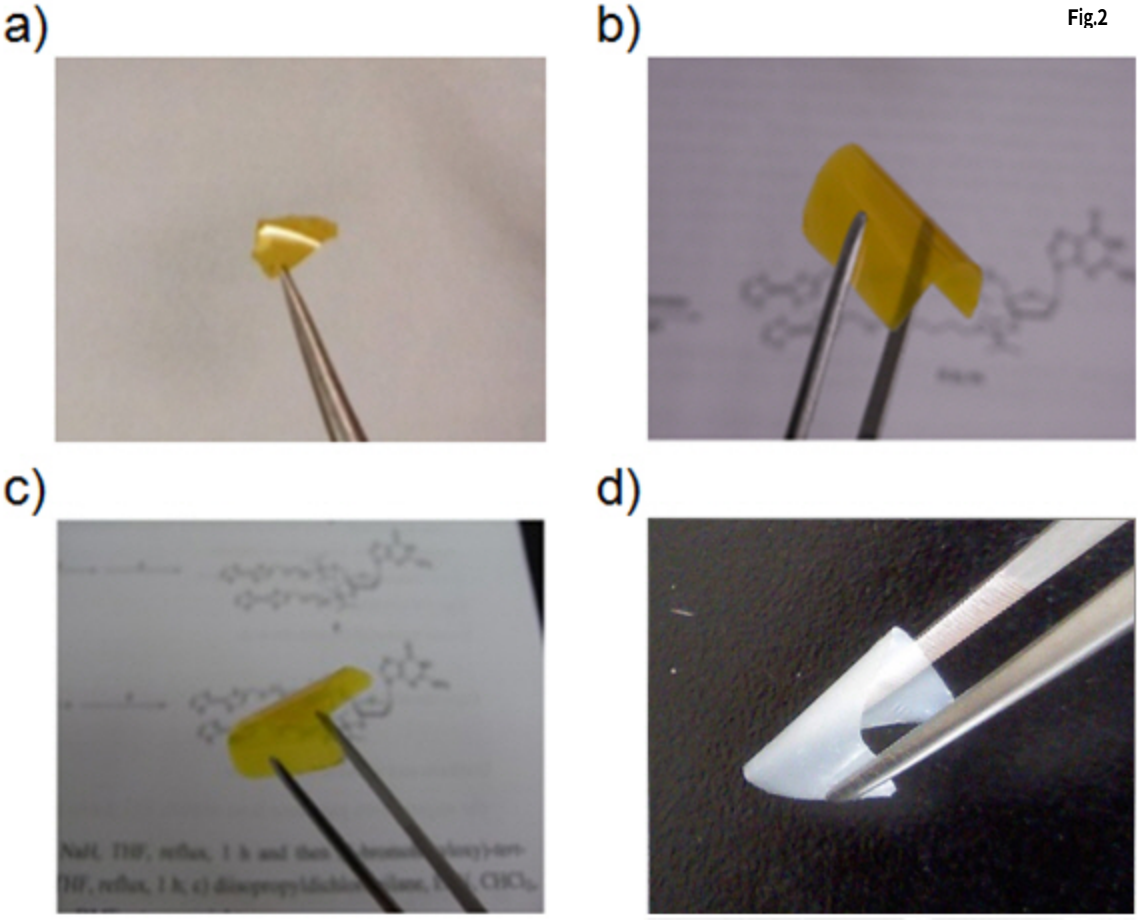

Fig.3

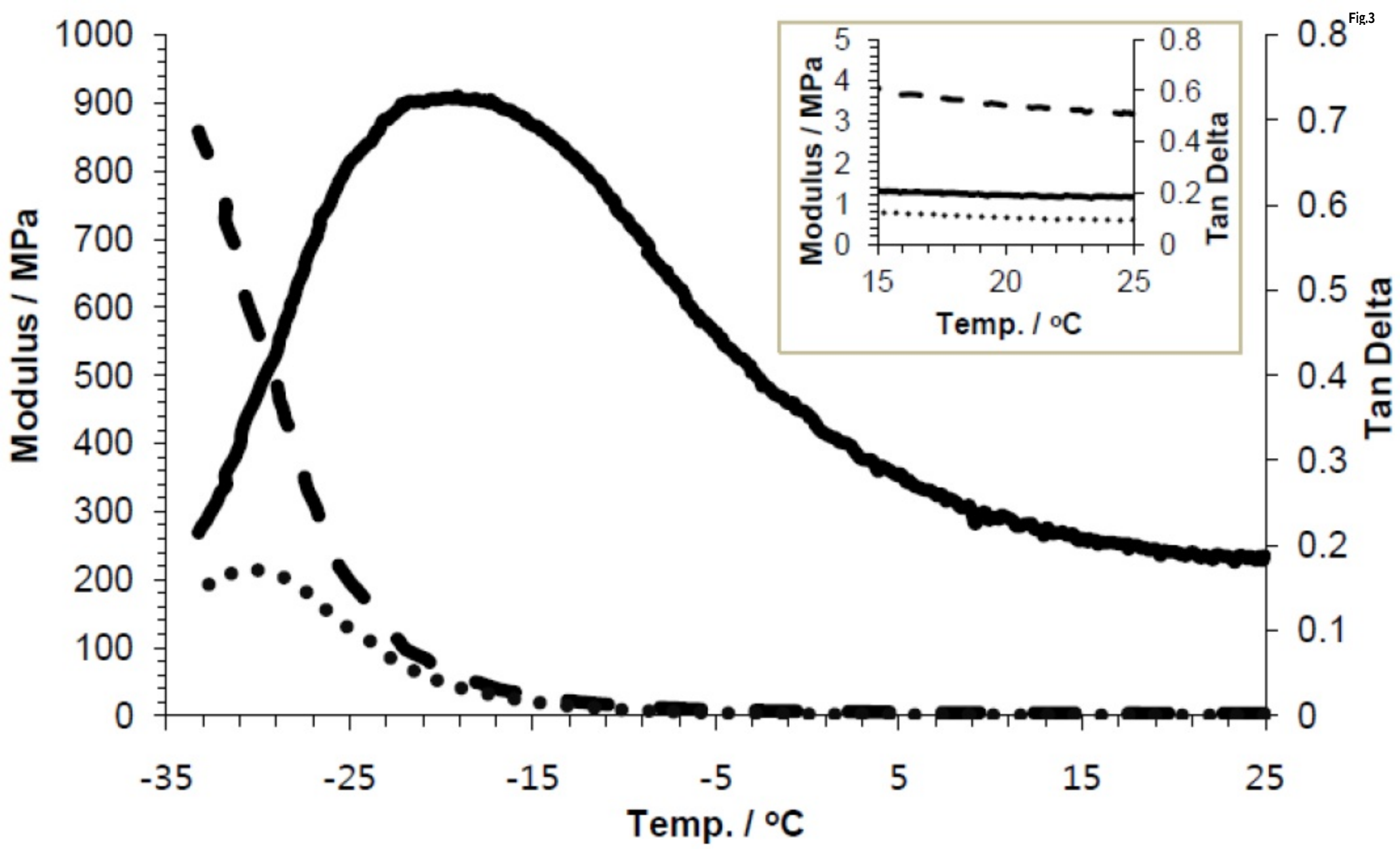
Modulus / MPa
Tan Delta
Temp. / °C
1000
900
800
700
600
500
400
300
200
100
0
0.8
0.7
0.6
0.5
0.4
0.3
0.2
0.1
-35
-25
-15
-5
5
15
25
Modulus / MPa
Tan Delta
Temp. / °C
5
4
3
2
1
0
0.8
0.6
0.4
0.2
0
15
20
25

Fig.4

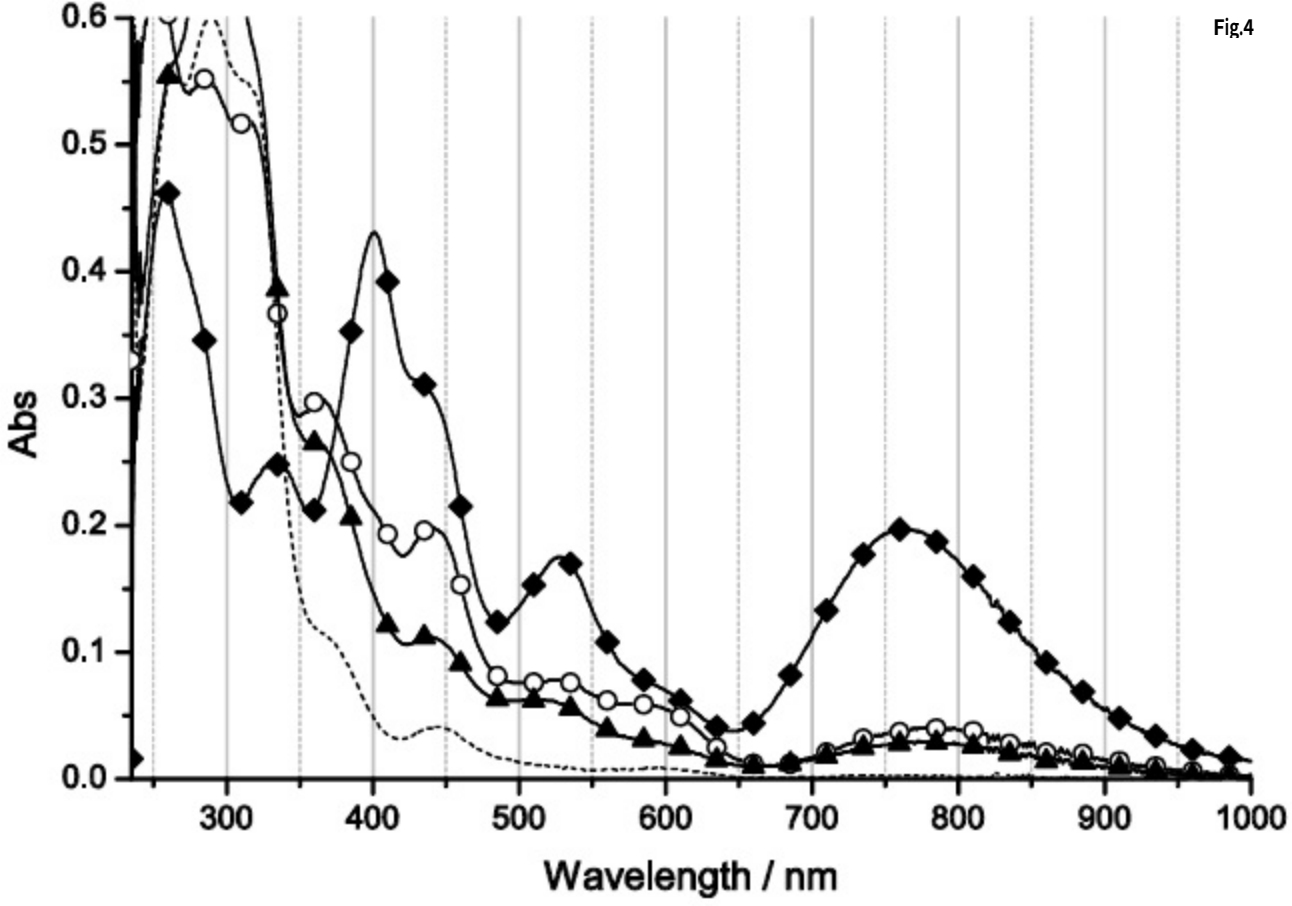
Abs
0.0
0.1
0.2
0.3
0.4
0.5
0.6
300
400
500
600
700
800
900
1000
Wavelength / nm

Fig.5

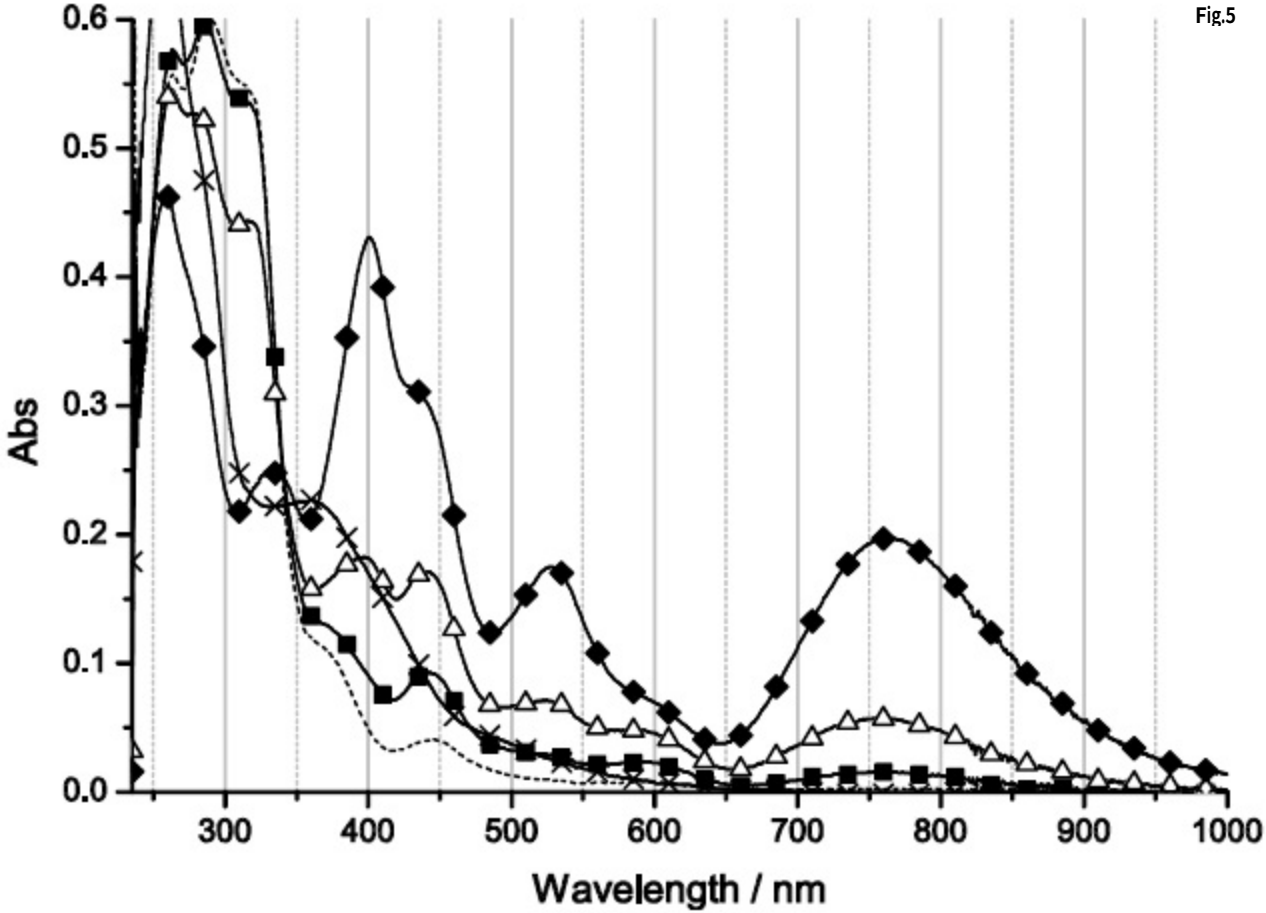
Abs
0.0
0.1
0.2
0.3
0.4
0.5
0.6
300
400
500
600
700
800
900
1000
Wavelength / nm

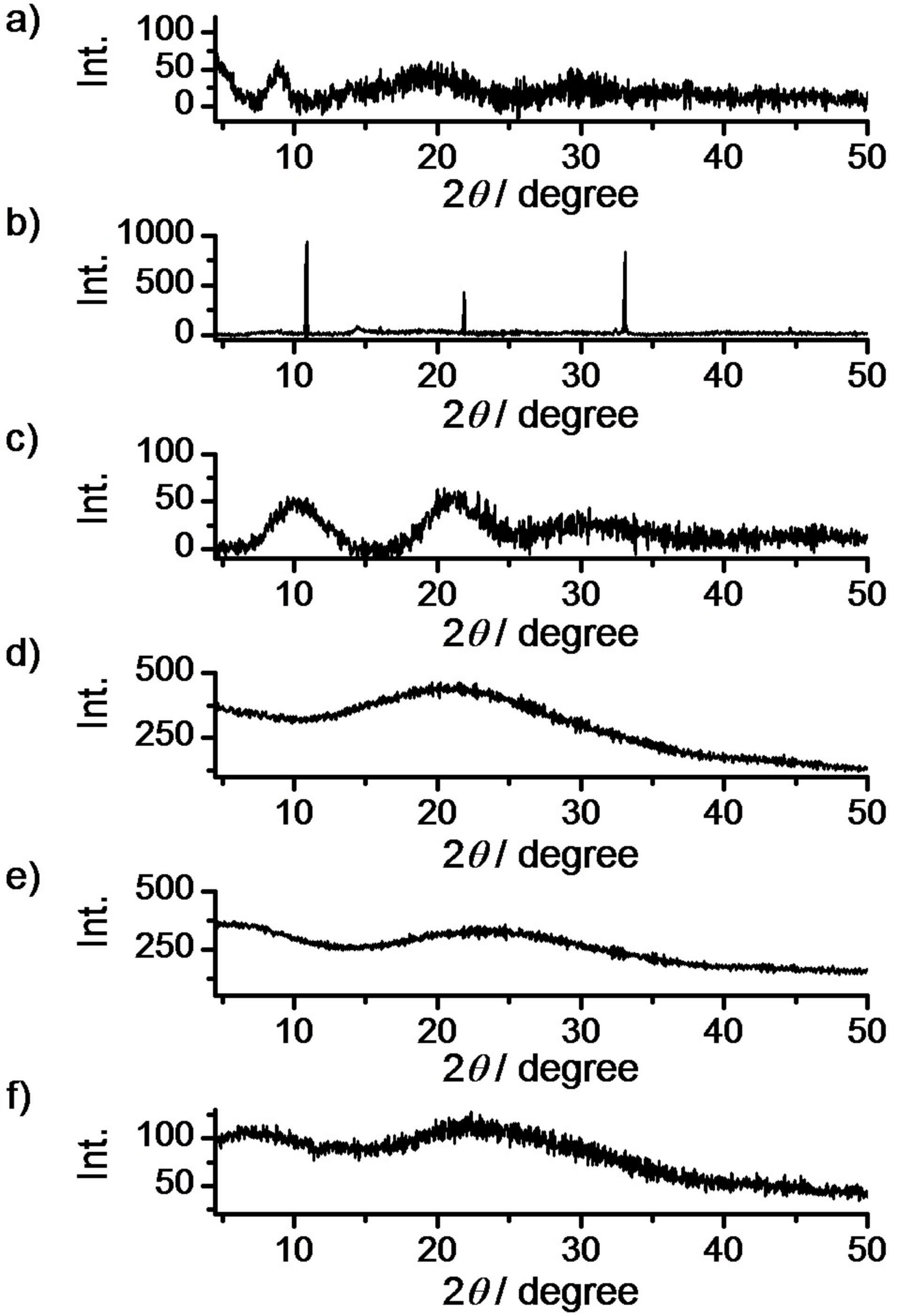
a)
Int.
100
50
0
10
20
30
40
50
2θ / degree
b)
Int.
1000
500
0
10
20
30
40
50
2θ / degree
c)
Int.
100
50
0
10
20
30
40
50
2θ / degree
d)
Int.
500
250
10
20
30
40
50
2θ / degree
e)
Int.
500
250
10
20
30
40
50
2θ / degree
f)
Int.
100
50
10
20
30
40
50
2θ / degree

Table 1 The thermal properties of derivatives **1-4**

Derivative	MW / g•mol^{-1}	$T_{d5\%}$ / °C [a]	T_{g2nd} / °C [b]	T_c / °C [c]	T_{m1st} / °C [d]	T_{m3rd} / °C [e]
1	960.5	225.4	-1.2	6.9	123	79.5
2	1161	241.1	-4.6	17	95.1	76.2
3	1361	256.4	-21.	21	75.2	74.7
4	696.1	249.9	-52	15	162	126

[a] Temperature for 5.0% thermal decomposition obtained by TGA (heating rate of 10 °C / min, argo n atmosphere), [b] Glass transition temperature obtained by DSC curve of second heating run, [c] Phas e transition temperature obtained by DSC of second heating run, [d] Melting point on the fist heatin g run of DSC, [e] Melting point on the third heating run of DSC.

Table 2 The mechanical properties of the films of derivatives **2-4**

Derivative	σ_E / MPa [a]	E / % [b]	E' / MPa [c]	E'' / MPa [d]	T_g / °C [e]	Tan δ [f]
2	1.2	23	8.28	1.49	-3.7	0.6
3	0.19	20	3.19	0.599	-19	0.7
4	2.5	2.7	184	4.69	-51	0.2

[a] Tensile strength of self-supporting film, [b] Elongation of break point in tensile test, [c] Storage modulus (E') at 25 °C, [d] Loss modulus (E'') at 25 °C, [e] Glass transition temperature obtained by DMA, [f] Tan δ (= E'' / E') at glass transition temperature.

Table 3 Electrical conductivities of derivatives **1-3**

Entry	Oxidant	[Ox] / [derivatives]	Electrical conductivity ($S \cdot cm^{-1}$)[a]		
			1	2	3
1[b]	none	0	nd[d]	nd	nd
2[b]	TCNQ	2	nd	1.00×10^{-2}	3.66×10^{-2}
3[b]	TCNQ	1	nd	2.51×10^{-3}	9.35×10^{-4}
4[b]	TCNQ	3	nd	1.81×10^{-3}	7.05×10^{-4}
5[b]	TCNE	2	nd	nd	nd
6[b]	I_2	2	nd	nd	nd
7	$NOBF_4$	2	nd	nd	nd
8	$FeCl_3$	2	nd	nd	nd
9	$AgBF_4$	2	nd	nd	nd
10	Fe^{3+} [c]	2	nd	nd	nd

[a] Electrical conductivity of the cast film from THF solution was determined by two-probe technique at room temperature, [b] Previous work, [c] Acetylferrocenium tetrafluoroborate, [d] Not determined due to low electrical conductivity.